- Supporting Information -

Solvent-free powder synthesis and MOF-CVD thin films of the large-pore metal-organic framework MAF-6

Timothée Stassin,[†] Ivo Stassen,[†] João Marreiros,[†] Alexander John Cruz,[†] Rhea Verbeke,[†] Min Tu,[†] Helge Reinsch,[‖] Marcel Dickmann,[‡] Werner Egger,[§] Ivo F. J. Vankelecom,[†] Dirk E. De Vos,[†] Rob Ameloot*[,†]

[†]Centre for Membrane Separations, Adsorption, Catalysis and Spectroscopy for Sustainable Solutions (cMACS), KU Leuven, Celestijnenlaan 200F box 2454, 3001 Leuven, Belgium.

[‖]Institut für Anorganische Chemie, Christian-Albrechts-Universität, Max-Eyth-Straße 2, 24118 Kiel, Germany.

[‡]Heinz Maier-Leibnitz Zentrum (MLZ) and Physik Department E21, Technische Universität München, Lichtenbergstraße 1, 85748 Garching, Germany.

[§]Institut fur Angewandte Physik und Messtechnik LRT2, Universität der Bundeswehr München, Werner-Heisenberg-Weg 39, 85577 Neubiberg, Germany.

Correspondence to:

Prof. Dr. Rob Ameloot
Tel.: +32-1637-6674
Email: rob.ameloot@kuleuven.be

Contents

S1. Materials and methods

Materials and methods can be found in the manuscript.

S2. Solvent-free synthesis of MAF-6 and ZIF-8 at room conditions

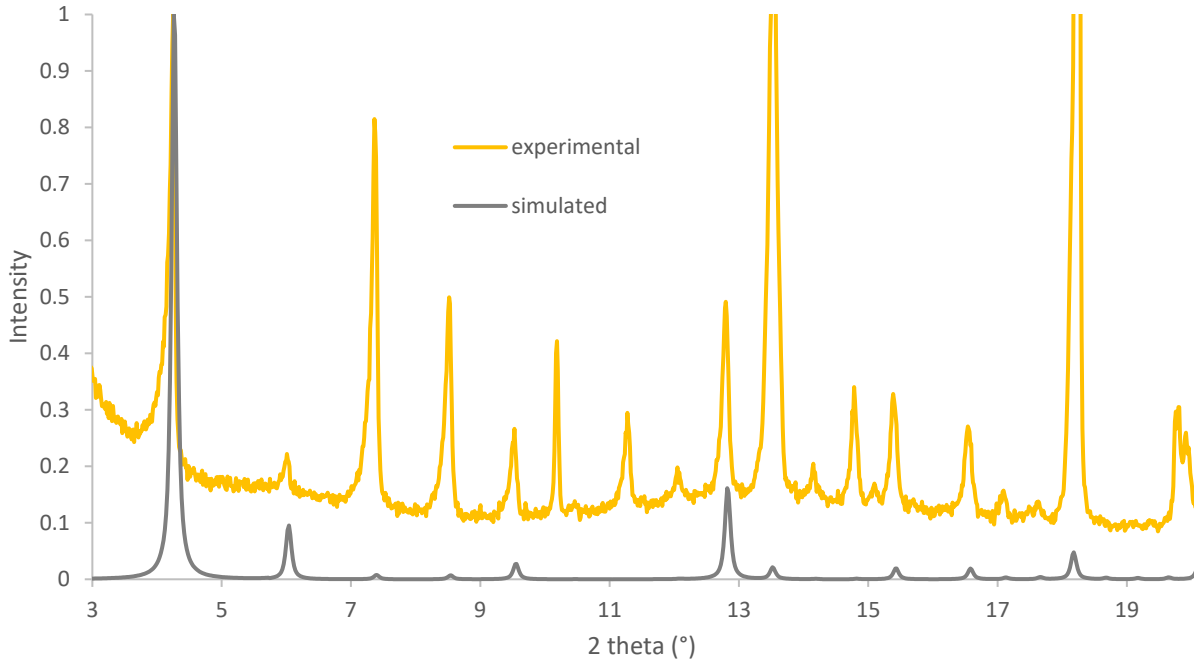

Figure S2.1. Powder X-ray diffractogram of a ZnO:HeIm physical mixture after 7 days aging in a closed vessel at room conditions (yellow, 25 °C, 60% RH), and simulated pattern for MAF-6 (grey). Additional reflections corresponding to unreacted HeIm linker molecules can also be observed.

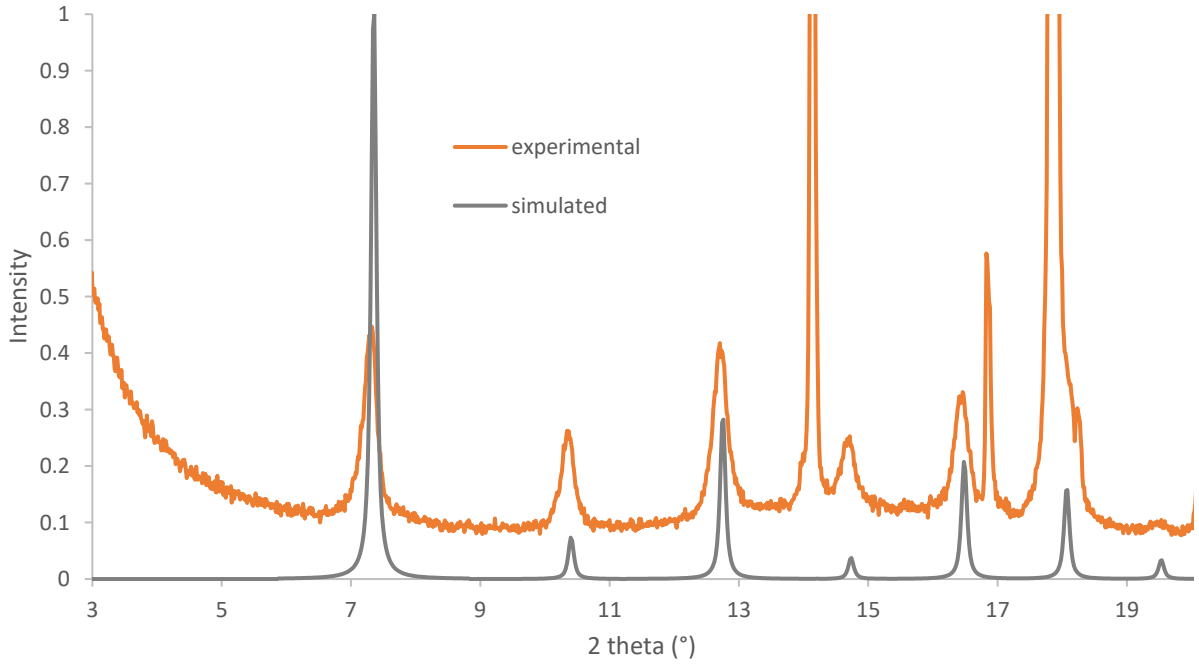

Figure S2.2. Powder X-ray diffractogram of a ZnO:HmeIm physical mixture after 7 days aging in a closed vessel at room conditions (orange, 25 °C, 60% RH), and simulated pattern for ZIF-8 (grey). Additional reflections corresponding to unreacted HmIm linker molecules can also be observed.

S3. MAF-6 Rietveld refinement and crystallographic information

Rietveld refinement

The PXRD pattern of the obtained MAF-6 matches very well with the expected cubic symmetry (space group *Pm*-3*m)* of ZIF-71, which is an isoreticular MOF based on Zn^{2+} and 4,5-dichloroimidazole also exhibiting the RHO topology. Hence a model of MAF-6 with primitive cubic symmetry was developed using Materials Studio.[1] The linker molecules in ZIF-71 were replaced by 2-ethylimidazole and the indexed cell parameters were superimposed, following energetic optimization by force field calculations using the universal force field[2] as implemented in the forcite routine of Materials Studio. This model was refined by Rietveld methods using Topas Academics.[3] For the refinement, diffraction data were collected at the Advanced Photon Source at Argonne National Laboratory, United States of America. All atoms were freely refined using only distance restraints. The background was modelled as 24th order polynomial and the shape of the peaks was modelled by a Pseudo Voigt function. The temperature factors were refined for zinc and linker molecules as two different parameters. Zinc oxide was refined as minor phase (32.4(1) wt%). In addition one peak at 3.48° 2θ, likely originating from residual linker, was refined as single peak. The final plot is shown in Figure S3.1 and the most relevant parameters are summarized in Table S3.1.

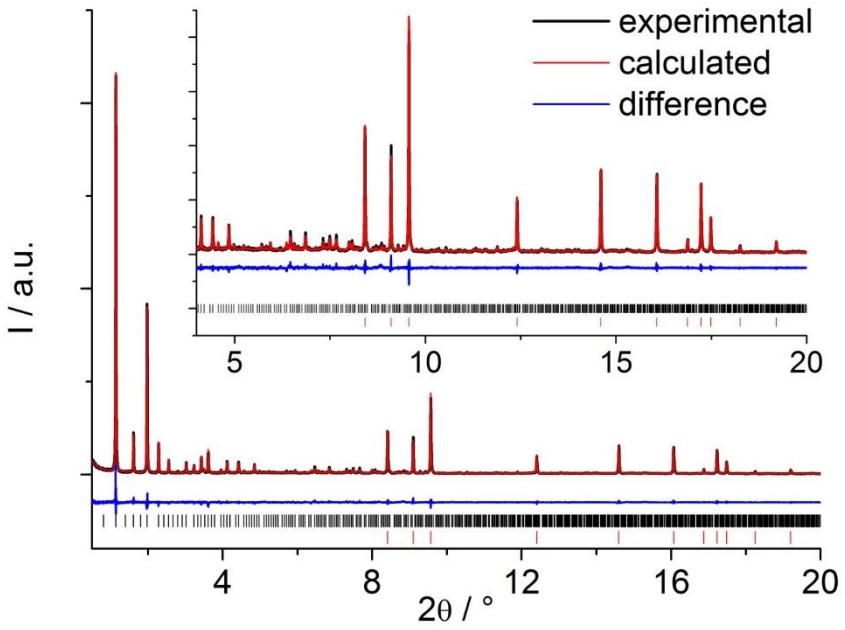

Figure S3.1. Rietveld refinement plot of MAF-6 (λ = 0.412703 Å). The black line is the experimental data, the red line gives the fit and the blue line indicates the difference. Black vertical bars mark the allowed reflection positions, red bars indicate peaks for hexagonal ZnO.

Table S3.1. Relevant parameters for the Rietveld refinement of MAF-6.

formula	$Zn(C_5N_2H_7)_2$
crystal system	Cubic
space group	*Pm*-3*m*
$a = b = c$ / Å	29.2944(3)
$\alpha = \beta = \gamma$ / °	90
V/ Å^3	25139.4(9)
R_{wp} / %	9.6
R_{Exp} / %	8.1
R_{Bragg} / %	3.9
GoF	1.2

Crystallographic information

The crystallographic information file was deposited at the Cambridge Crystallographic Data Centre where it can be accessed free of charge.

S4. ^{1}H NMR spectroscopy

The linker concentration in the digested mixture was derived from the ratio of the eIm protons to the TMAB protons in the ^{1}H NMR spectrum (Figure S4.1). The linker concentration in the digested mixture could then be converted to a linker weight fraction $wt\%_{eIm}$ in the activated sample knowing the digestion volume V and activated sample mass m_{sample}. The MAF-6 weight fraction $wt\%_{MAF}$ in the activated sample could eventually be calculated using the structure formula [Zn(eIm)$_2$] and the remaining content $wt\%_{ZnO}$ assumed to be ZnO.

$$C_{eIm} = \frac{\frac{I_{CH_3}}{3}}{\frac{I_{TMAB}}{12}} * C_{TMAB}$$

$$wt\%_{eIm} = \frac{C_{eIm} * V * M_{eIm}}{m_{sample}}$$

$$wt\%_{MAF} = (1 + \frac{M_{Zn}}{2 * M_{eIm}}) * wt\%_{eIm}$$

$$wt\%_{ZnO} = 1 - wt\%_{MAF}$$

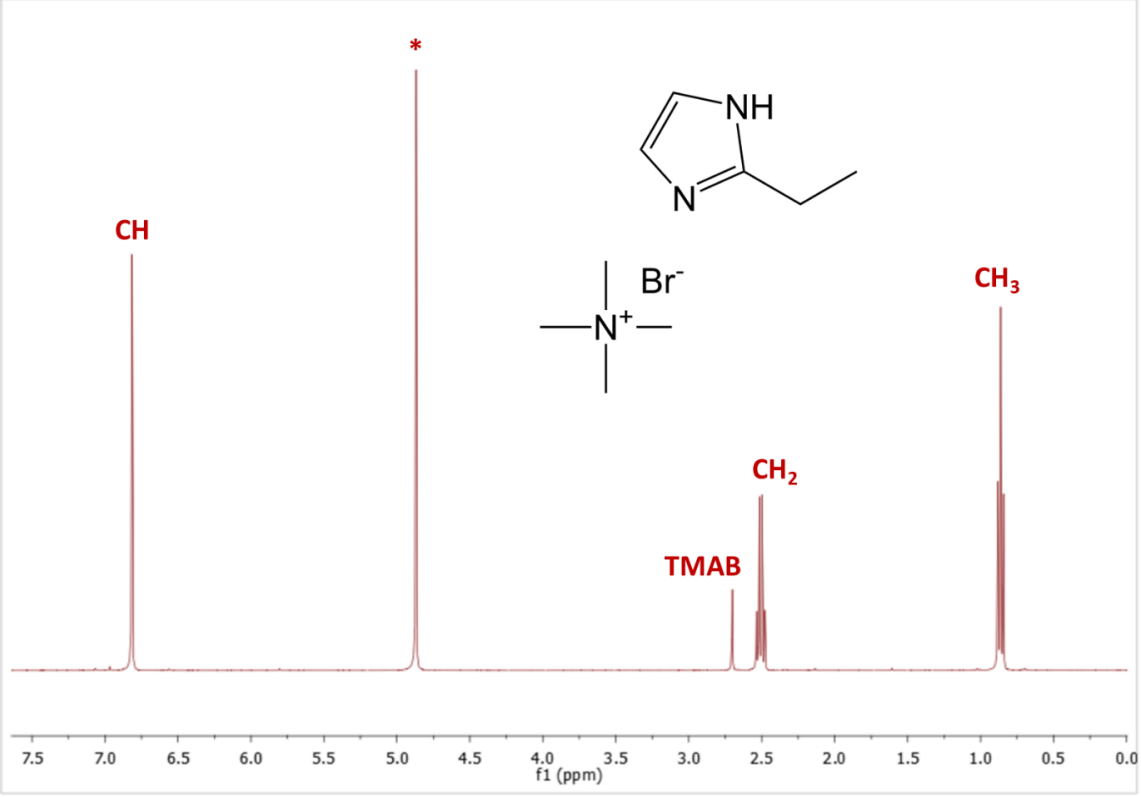

Figure S4.1. ^{1}H NMR spectrum of digested MAF-6 using tetramethylammonium bromide (TMAB) as quantification standard. Spectrum details: ^{1}H NMR (400 MHz, D_2O) δ 6.81 (s, 2H, C**H**), 2.70 (s, 12H, C**H$_3$**), 2.51 (q, *J* = 7.7 Hz, 2H, C**H$_2$**), 0.86 (t, *J* = 7.7 Hz, 3H, C**H$_3$**).

S5. SEM images of MAF-6 powder

MAF-6 from 25 nm ZnO nanoparticles

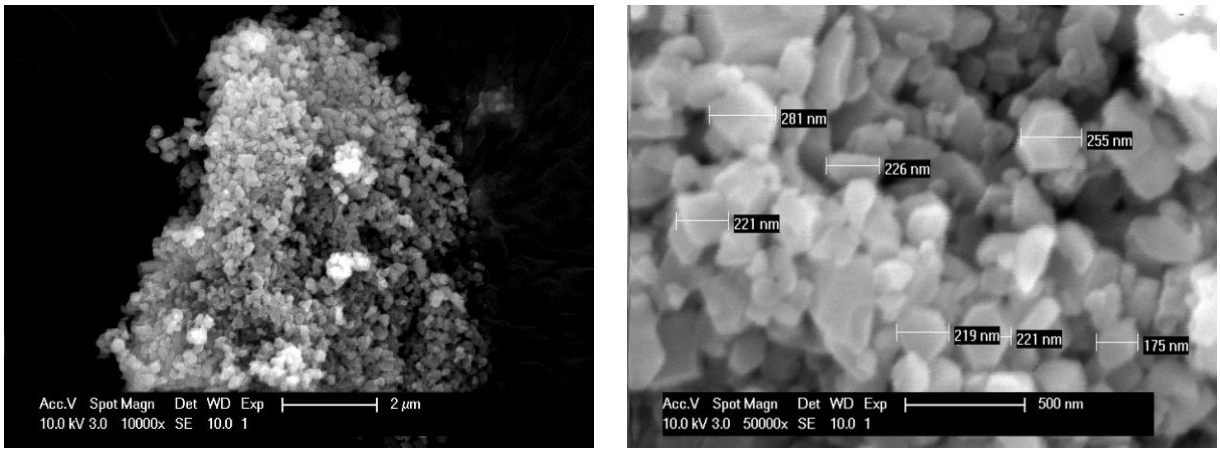

MAF-6 from micron-sized ZnO particles

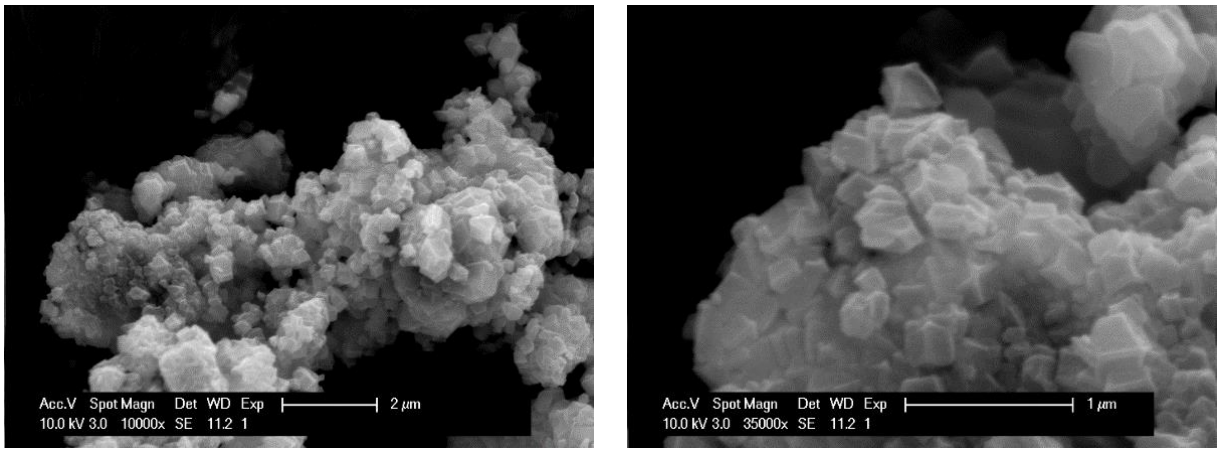

Figure S5.1. SEM images of MAF-6 powder prepared via solvent-free synthesis at 80 °C for 24 h from < 50 nm ZnO nanoparticles (top) and micron-sized ZnO particles (bottom).

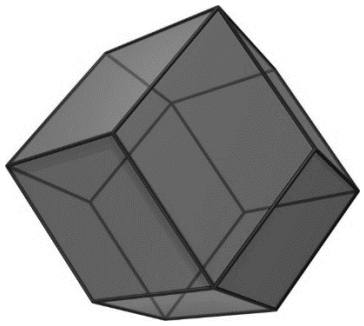

Figure S5.2. Rhombic dodecahedron.

S6. Volume expansion upon ZnO-to-MOF conversion

Definitions

Table S6.1. Symbols unit and definition for ZnO-to-MF-OF volume expansion coefficient derivation.

Symbol	Unit	Definition
$V_{ZnO,start}$	Å³	The starting ZnO volume
$V_{ZnO,end}$	Å³	The residual ZnO volume
V_{MOF}	Å³	The grown MOF volume
$C_{Zn,ZnO}$	Ion Å^{-3}	The Zn ion crystallographic density in the ZnO phase
$C_{Zn,MOF}$	Ion Å^{-3}	The Zn ion crystallographic density in the ZnO phase
$n_{Zn,ZnO,start}$	Ion	The number of Zn ions initially in the ZnO phase
$n_{Zn,ZnO,end}$	Ion	The number of Zn ions in the residual ZnO phase
$n_{Zn,MOF}$	Ion	The number of Zn ions in the grown MOF phase

Zn ions mass balance

Assuming pristine ZnO, so all the Zn is initially present in the ZnO phase, the following Zn balances are applicable:

$$n_{Zn,ZnO,start} = n_{Zn,MOF} + n_{Zn,ZnO,end}$$

$$V_{ZnO,start} * C_{Zn,ZnO} = V_{MOF} * C_{Zn,MOF} + V_{ZnO,end} * C_{Zn,ZnO}$$

Spherical particles (3D) expansion

If the ZnO-to-MOF conversion is complete, i.e. $V_{ZnO,end} = 0$, and with d_{ZnO} the diameter of the initial ZnO spherical particle, d_{MOF} the diameter of the final MOF spherical particle, and X_{sphere} the expansion coefficient for spherical particles:

$$d_{MOF} = d_{ZnO} * X_{sphere}$$

$$X_{sphere} = \sqrt[3]{\frac{C_{Zn,ZnO}}{C_{Zn,MOF}}}$$

If the ZnO-to-MOF conversion is incomplete, i.e. $V_{ZnO,start} > V_{ZnO,end} > 0$ with R the degree of Zn conversion:

$$R = \frac{n_{Zn,MOF}}{n_{Zn,ZnO,start}}$$

and assuming a spherical residual ZnO core with diameter $d_{ZnO,core}$ surrounded by a spherical MOF shell, with total MOF@ZnO core-shell spherical particle diameter $d_{MOF@ZnO}$:

$$V_{ZnO,core} = \frac{R * n_{Zn,ZnO,start}}{C_{Zn,ZnO}}$$

$$V_{MOF,shell} = \frac{(1-R) * n_{Zn,ZnO,start}}{C_{Zn,MOF}}$$

$$d_{ZnO,core} = \sqrt[3]{\frac{6}{\pi} * V_{ZnO,core}}$$

$$V_{MOF@ZnO} = V_{MOF,shell} + V_{ZnO,core}$$

$$d_{MOF@ZnO} = \sqrt[3]{\frac{6}{\pi} * (V_{MOF,shell} + V_{ZnO,core})}$$

Film (1D) expansion, full conversion

If the ZnO-to-MOF conversion is complete, i.e. $V_{ZnO,end} = 0$, and with t_{ZnO} the thickness of the initial ZnO film, t_{MOF} the thickness of the final MOF film, and X_{film} the film expansion coefficient:

$$t_{MOF} = t_{ZnO} * X_{film}$$

$$X_{film} = \frac{C_{Zn,ZnO}}{C_{Zn,MOF}}$$

Expansion coefficients

Table S6.2 Spherical (3D) and film (1D) expansion coefficients calculated for complete ZnO-to-ZIF-8 and -MAF-6 conversion from crystalline ZnO with a nominal density of 5.61 g cm^{-3} and ALD ZnO with a measured ZnO density of 3.9 g cm^{-3}.[4]

MOF	X_{sphere} ZnO (5.61 g cm^{-3})	X_{film} ZnO (5.61 g cm^{-3})	X_{film} ALD ZnO (3.9 g cm^{-3})
ZIF-8 (CSD code: VELVOY)	2.57	17	12
MAF-6 (this work)	2.79	22	15

S7. N_2 physisorption

Table S7.1. Porosimetry results extracted from nitrogen physisorption isotherms measured at -196 °C (77 K) on MAF-6 powders synthesized from ZnO nanoparticles and micron-sized particles. The total surface area is calculated using the Brunauer-Emmett-Teller equation, the external surface area using the t-plot method, and the pore surface area by subtracting the external surface area from the total surface area. The wt% MAF-6 in the sample as determined by TGA is used to correct the pore surface area for the MAF-6 content. The surface area obtained from simulations for a protonated structure using Materials Studio.[1] Literature values are given for comparison.

	MAF-6 from ZnO nanoparticles	**MAF-6 from micron-sized particles**
Total surface area (BET)	1451 $m^2 g^{-1}$	1015 $m^2 g^{-1}$
External surface area (t-plot)	85 $m^2 g^{-1}$	57 $m^2 g^{-1}$
Pore surface area	1366 $m^2 g^{-1}$	958 $m^2 g^{-1}$
Corrected pore surface area (TGA)	**1485 $m^2 g^{-1}_{MAF}$**	**1474 $m^2 g^{-1}_{MAF}$**
Simulated surface area	1571 $m^2 g^{-1}_{MAF}$	1571 $m^2 g^{-1}_{MAF}$

Solvothermal MAF-6[5]	BET surface area	1343 $m^2 g^{-1}_{MAF}$
MAF-6 prepared by accelerated aging[6]	BET surface area	1241 $m^2 g^{-1}_{MAF}$

S8. Activation: removal of residual linker filling the pores

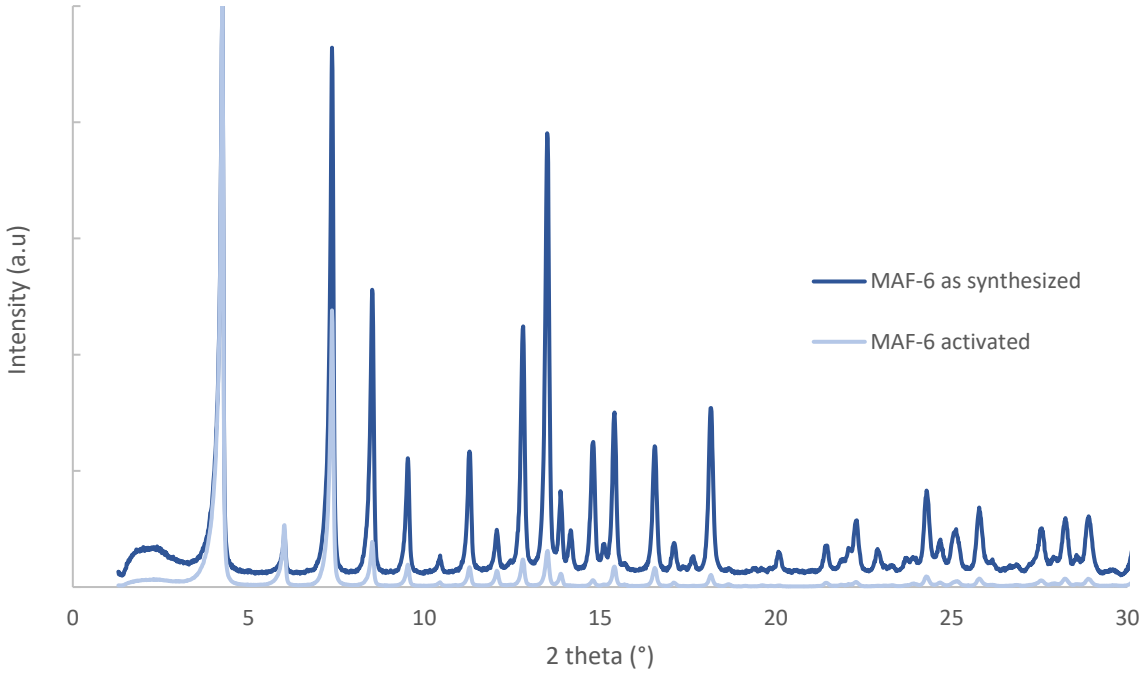

Figure S8.1. Activation of as-synthesized MAF-6 goes paired with significant changes in diffracted intensity, indicative of pore evacuation from residual HeIm linker molecules. Powder X-ray diffractogram of MAF-6 as-synthesized (dark) and MAF-6 after activation (light).

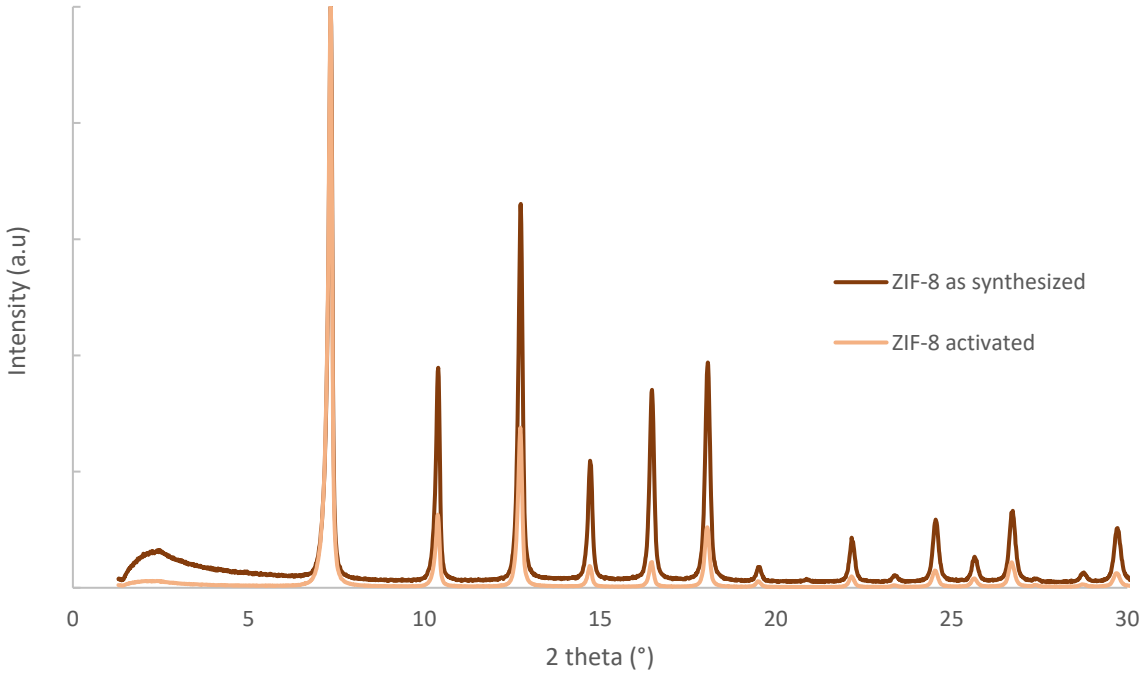

Figure S8.2. Activation of as-synthesized ZIF-8 goes paired with significant changes in diffracted intensity, indicative of pore evacuation from residual HmIm linker molecules. Powder X-ray diffractogram of ZIF-8 as synthesized (dark) and ZIF-8 after activation (light).

S9. EXAFS

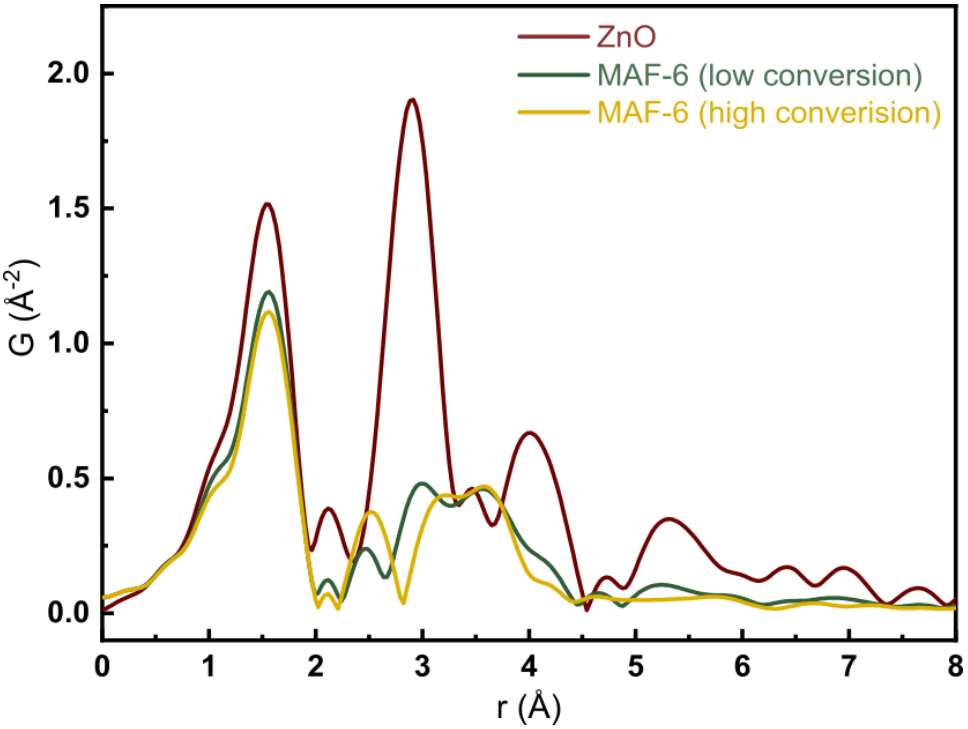

Figure S9.1. FT EXAFS of ZnO (red), a sample with a high degree of ZnO-to-MAF-6 conversion (yellow), and a sample with low degree of ZnO-to-MAF-6 conversion prepared at a lower temperature (green).

S10. Total scattering

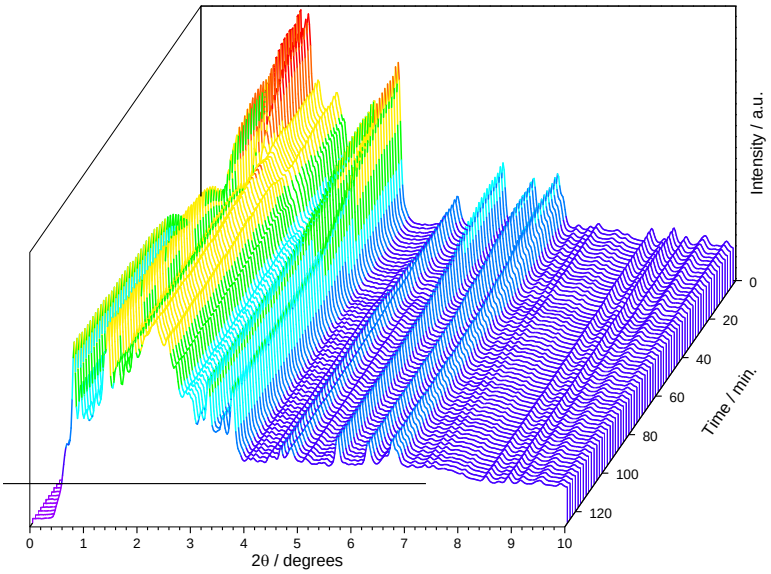

Figure S10.1 Total scattering patterns of MAF-6 prepared *in situ*.

S11. ATR-FTIR

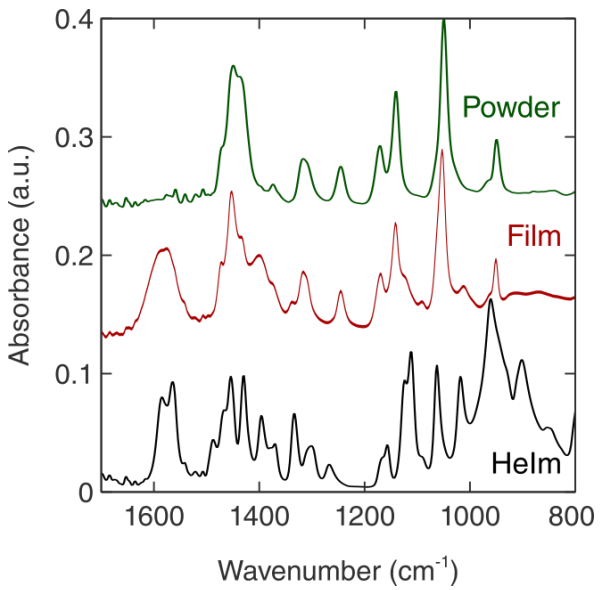

Figure S11.1. ATR-FTIR spectra of MAF-6 powder (green), MAF-6 film (red) and HeIm powder (black).

S12. Positron Annihilation Lifetime Spectroscopy (PALS)

Positronium lifetimes and intensities

Table S12.1. Results of the PALS measurements performed on a MAF-6 film (top) and powder pellet (bottom) at a positron implantation energy of 1.0 and 1.5 keV.

	Film					
	***o*-Ps short**			***o*-Ps long**		
Energy (keV)	**Lifetime (ns)**	**d (nm)**	**Intensity (%)**	**Lifetime (ns)**	**d (nm)**	**Intensity (%)**
1	2.11 ± 0.19	0.59 ± 0.03	1.03 ± 0.07	18.75 ± 0.11	1.96 ± 0.01	12.97 ± 0.03
1.5	2.81 ± 0.28	0.70 ± 0.04	0.91 ± 0.05	19.60 ± 0.15	2.01 ± 0.01	13.18 ± 0.04
	Powder pellet					
	***o*-Ps short**			***o*-Ps long**		
Energy (keV)	**Lifetime (ns)**	**d (nm)**	**Intensity (%)**	**Lifetime (ns)**	**d (nm)**	**Intensity (%)**
1	2.00 ± 0.02	0.57 ± 0.00	13.08 ± 0.18	19.69 ± 0.21	2.02 ± 0.01	6.68 ± 0.02
1.5	1.92 ± 0.02	0.56 ± 0.00	14.83 ± 0.15	19.97 ± 0.18	2.03 ±0.01	8.08 ± 0.02

Positron mean implantation depths

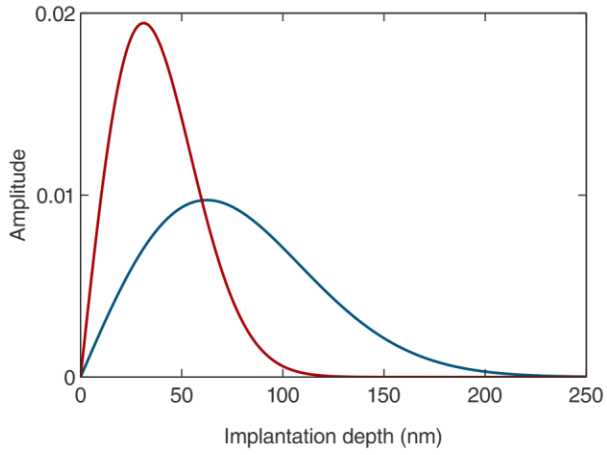

Figure S12.1. Positron implantation profiles in MAF-6 (crystallographic density = 0.77 cm^3 g^{-1}) calculated for a 1.0 keV (red) and 1.5 keV implantation energy (blue).

S13. Energy-dispersive X-ray spectroscopy (EDS)

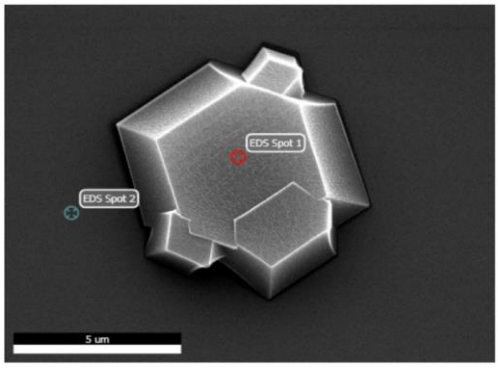

Figure S13.1. SEM image showing the location of the two EDS point measurements on a MAF-6 crystallite (spot 1) and near a MAF-6 crystallite (spot 2).

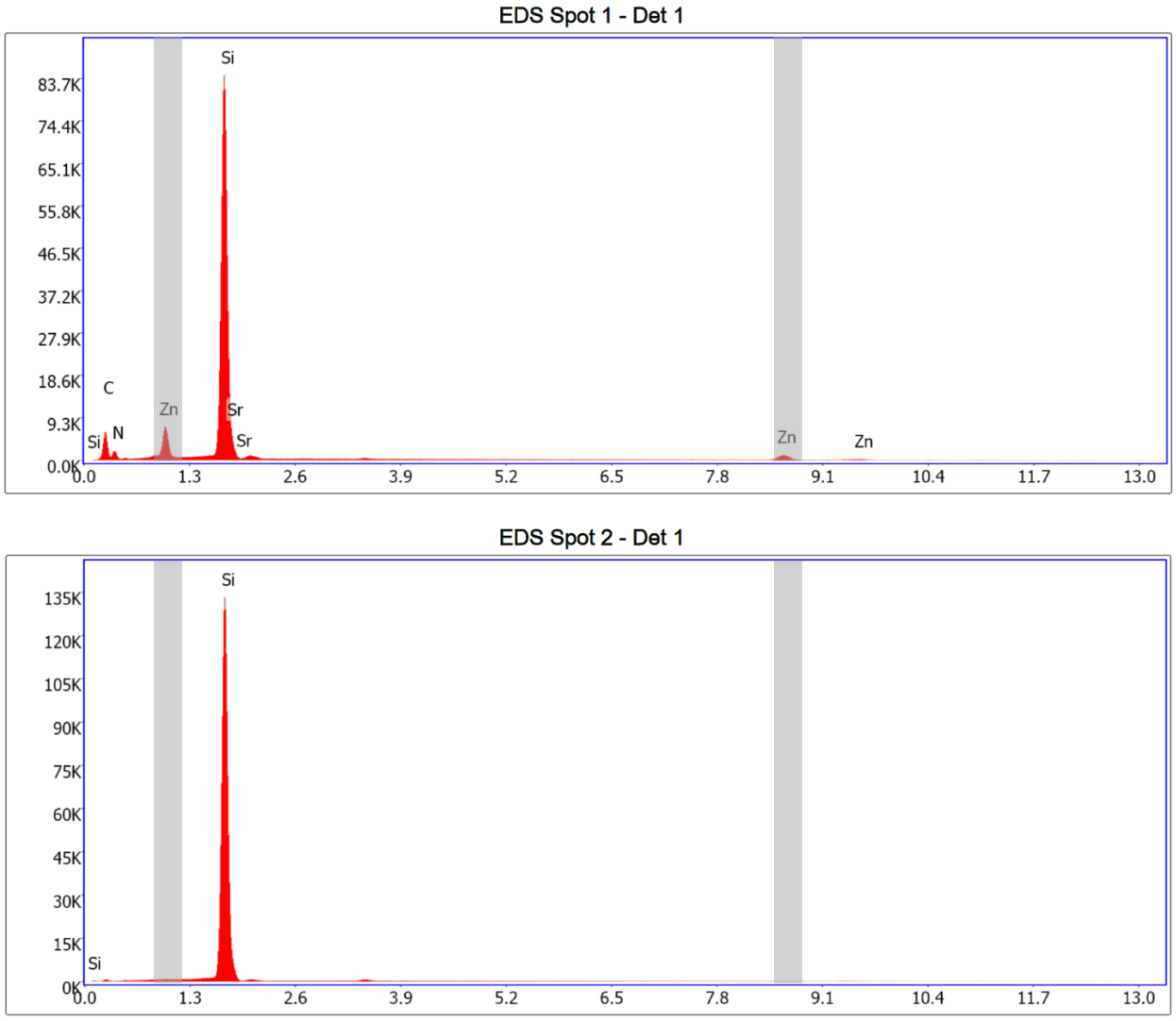

Figure S13.2. Raw EDS spectra and automatic assignment by the TEAM software for the two point measurements whose location is displayed in Figure S13.1. The ZnKα and ZnLα spectral lines are highlighted in grey. The Sr assignment should be neglected as the presence of this element in the sample is unlikely.

S14. SEM images of MAF-6 films

3 nm ZnO

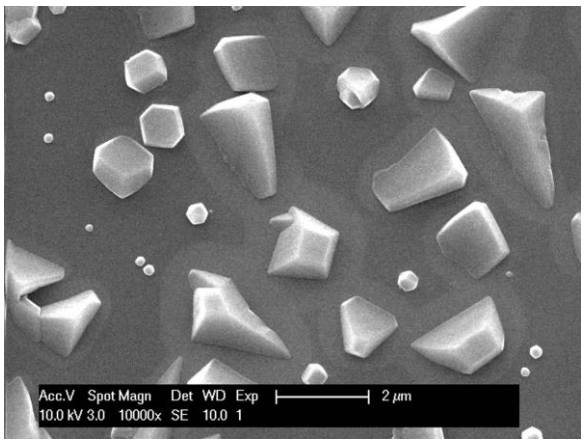

5 nm ZnO

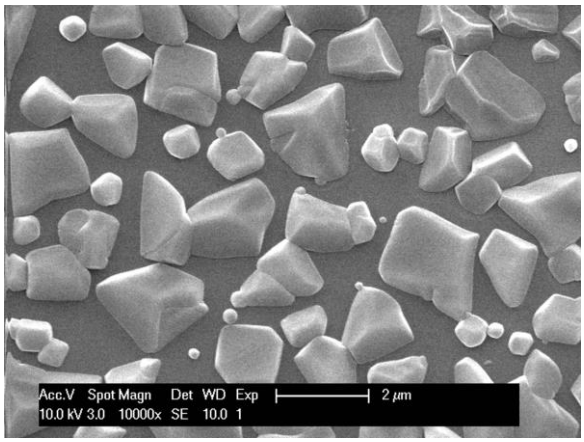

10 nm ZnO

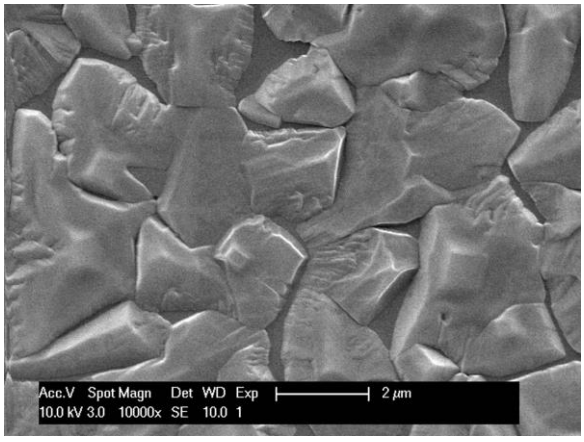

Figure S14.1. SEM images of MAF-6 films grown from 3 nm (top), 5 nm (middle) and 10 nm (bottom) ZnO layers under similar identical conditions.

S15. MAF-6 CVD: temperature gradient experiments

Tube furnace

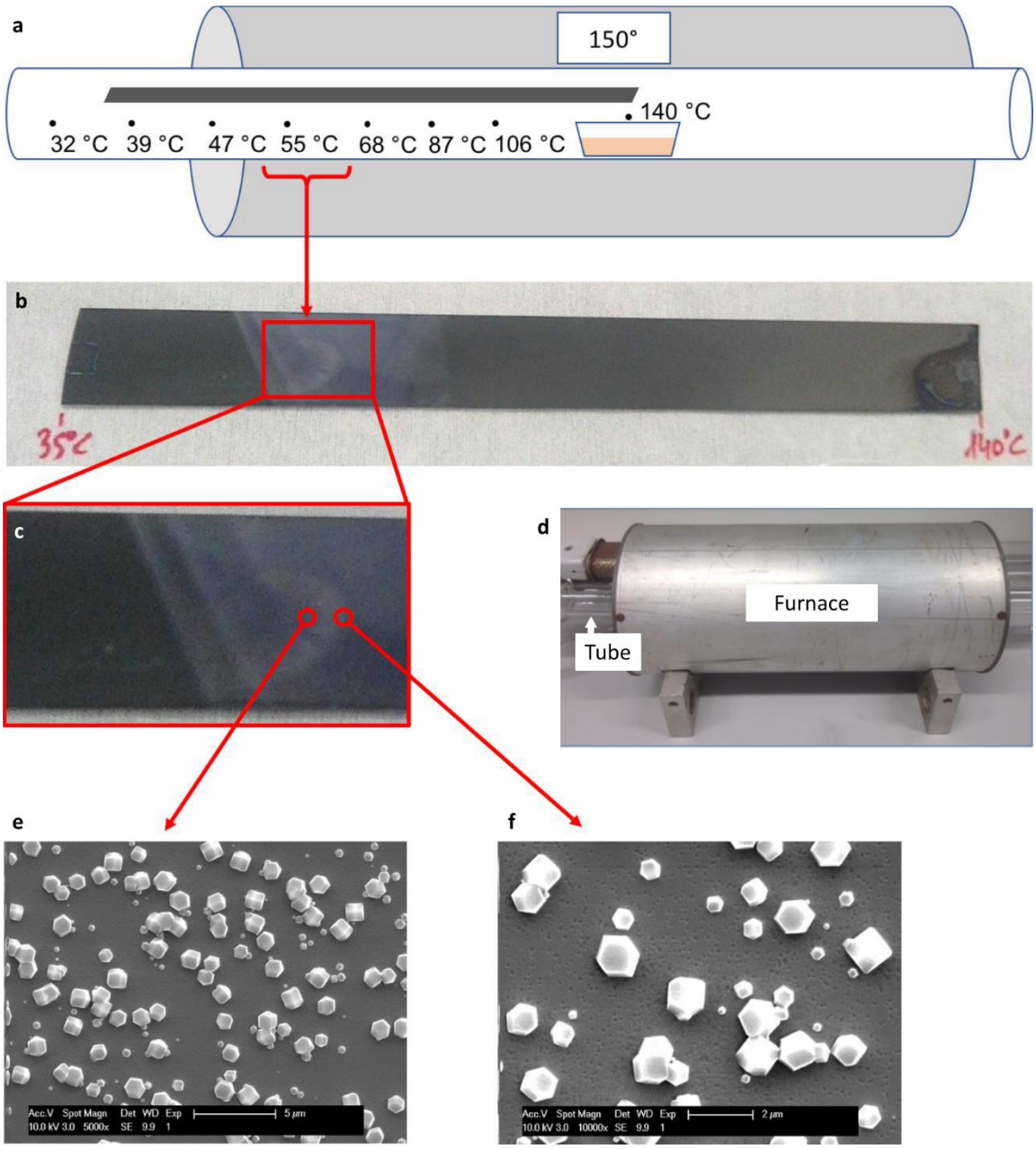

Figure S15.1. MAF-6 CVD using a tube furnace setup. **a**, Schematic representation of the experiment where the center region of the tube is heated to 150 °C while the tube end is at room temperature. A HeIm-containing boat is placed at the center of the tube (T = 140 °C) while a long ZnO wafer piece is placed in the tube, extending from the tube center to the tube end, thereby covering the whole temperature range from 140 °C to 35 °C. **b** and **c**, an image of the wafer piece after the experiment at two different magnifications. **d**, image of the tube furnace setup. **e** and **f**, SEM images of the only location along the wafer piece where MAF-6 growth was observed, corresponding to the temperature region of 50-65 °C.

Temperature-controlled reactor chamber

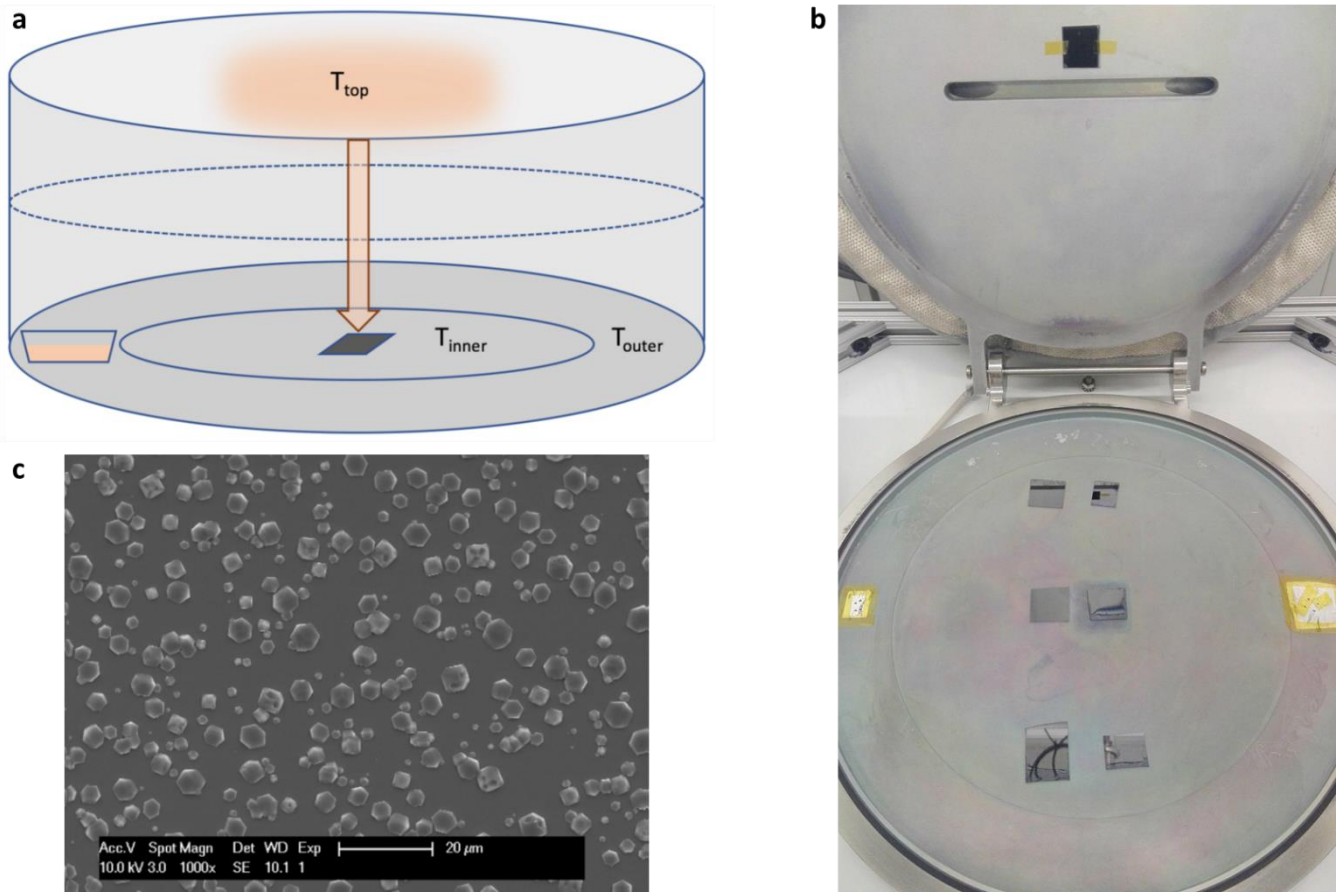

Figure S15.2. MAF-6 CVD using a temperature-controlled reactor chamber. **a**, Schematic representation of the experiment: HeIm is spread on the outer region of the chamber and a ZnO wafer piece is placed at the center of the chamber which has three independently controlled temperature regions: top (i.e., chamber lid, T= 150 °C), outer (T = 90 °C), and inner region (T = 80 °C). **b**, an image of the reactor chamber. **c**, SEM image of the sample at the end of the experiment, showing MAF-6 growth.

S16. Fluorescence emission spectra

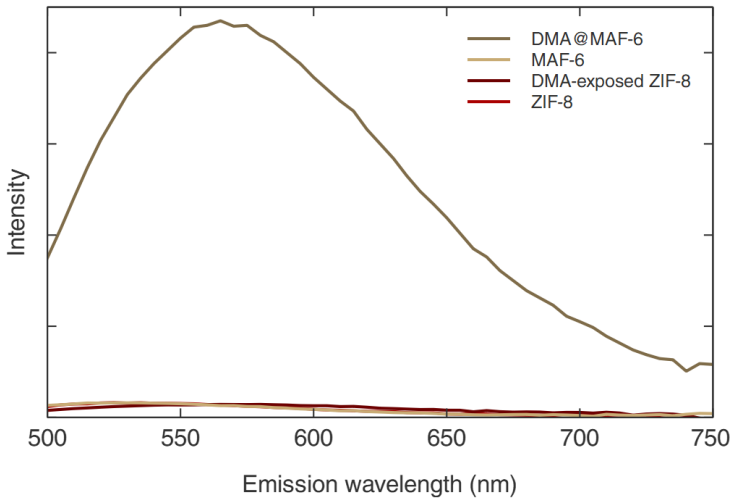

Figure S16.1. Fluorescence emission spectra of MAF-6, DMA@MAF-6, ZIF-8 and DMA-exposed ZIF-8 measured at an excitation wavelength of 475 nm.

S17. DMA@MAF-6 PXRD analysis

The pattern of MAF-6 loaded with 9,10-dimethylanthracene drastically changed peak intensities compared to pure MAF-6, but exhibits very similar peak positions. However, by indexing[3] it could be deduced that some slight deviations can be only explained by a subtle distortion of the cubic unit cell of MAF-6 to a tetragonal cell for MAF-6 loaded with 9,10-dimethylanthracene. A structure-less Pawley refinement was carried out using the extinction conditions suitable for space group symmetry *P*4/*mmm*. The final plot and the refined parameters are shown below. However, attempts to locate the guest molecules using a combination of modelling with Materials Studio[1] and Rietveld refinement did not succeed, indicating that the guest molecules are most likely arranged in a non-ordered fashion.

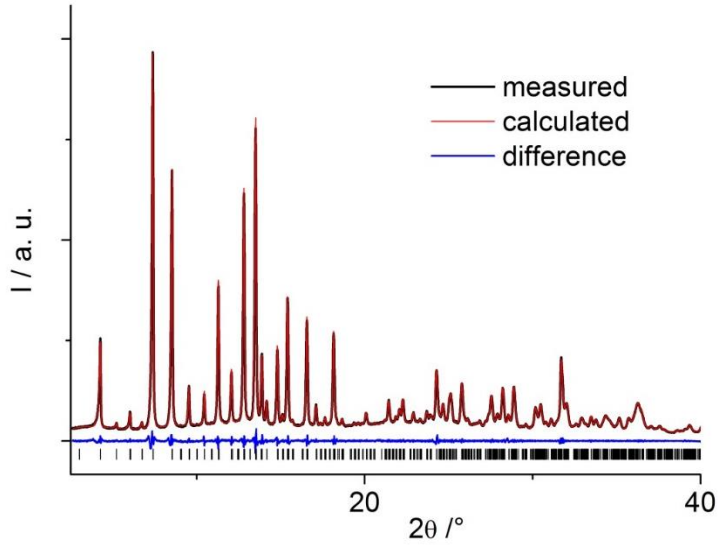

Figure S17.1. Structure-less Pawley refinement plot for MAF-6 loaded with 9,10-dimethylanthracene ($CuK_{\alpha1}$ radiation). The black line is the experimental data, the red line gives the fit and the blue line indicates the difference. Black vertical bars mark the allowed reflection positions.

Table S17.1. Some relevant parameters for MAF-6 loaded with dimethylanthracene.

crystal system	tetragonal
space group	*P*4/*mmm*
$a = b$ / Å	29.302(2)
c / Å	29.167(3)
$\alpha = \beta = \gamma$ / °	90
V/ Å^3	25042.5(9)
R_{wp} / %	3.1
R_{Exp} / %	1.5
GoF	2.0

S18. References

(1) *Materials Studio*; Accelrys, 2009.

(2) Rappe, A. K.; Casewit, C. J.; Colwell, K. S.; Goddard, W. A.; Skiff, W. M. UFF, a Full Periodic Table Force Field for Molecular Mechanics and Molecular Dynamics Simulations. *J. Am. Chem. Soc.* **1992**, *114* (25), 10024–10035. https://doi.org/10.1021/ja00051a040.

(3) *Topas Academics*; Coleho Software, 2007.

(4) *CRC Handbook of Chemistry and Physics: A Ready-Reference Book of Chemical and Physical Data*, 84th ed.; Chemical Rubber Company, Lide, D. R., Eds.; CRC Press: Boca Raton, 2003.

(5) He, C.-T.; Jiang, L.; Ye, Z.-M.; Krishna, R.; Zhong, Z.-S.; Liao, P.-Q.; Xu, J.; Ouyang, G.; Zhang, J.-P.; Chen, X.-M. Exceptional Hydrophobicity of a Large-Pore Metal–Organic Zeolite. *J. Am. Chem. Soc.* **2015**, *137* (22), 7217–7223. https://doi.org/10.1021/jacs.5b03727.

(6) Mottillo, C.; Lu, Y.; Pham, M.-H.; Cliffe, M. J.; Do, T.-O.; Friščić, T. Mineral Neogenesis as an Inspiration for Mild, Solvent-Free Synthesis of Bulk Microporous Metal–organic Frameworks from Metal (Zn, Co) Oxides. *Green Chem.* **2013**, *15* (8), 2121–2131. https://doi.org/10.1039/C3GC40520F.